FAILURE ANALYSIS OF HAUL TRUCK FINAL DRIVE GEARS

Rachman Setiawan, Budi Hartono Setiamarga, Bambang Widyanto

Fakultas Teknik Mesin & Dirgantara ITB,
Gd. Labtek II, Jl. Ganesha 10, Bandung 40132

Phone: +62-22-2500979, e-mail: rachmans@edc.ms.itb.ac.id

ABSTRACT

During their operational life, sometimes mechanical equipment experience failures. The failure often cause substantial loss of production opportunity. In order to prevent such failure from happening in the future, failure analysis activity needs to be carried out. It involves material and mechanical examination that yields the root cause of failure and the recommendation/mitigation plan, as a part of continuous improvement cycle within the industry. In one occassion, ring gears of the final drive belonging to a number of haul trucks experience breakage failure, causing major loss of production in a coal mining company. From Optical Emission Spectroscopy, it is found that the ring gear is made of AISI4340 high strength steel. It is a part of two-stage planetary gear in the final drive. A set of failure analysis activities was carried out, involving both material and mechanical examination. As a result, the root cause of failure was found to be a flaw in furnace and heat-treatment process accompanied by poor quality control.

Keywords: Failure analysis, Gears, Heavy equipment

1. Introduction

As a major coal mining company in the world, PT Kaltim Prima Coal (KPC) relies on their heavy duty dump trucks for hauling both overburden (OB) and coal from and to various places across the mining area. The dump trucks serve as a backbone of the company coal production, and their reliability and availability affects the continuity of production much. The maintanance cost of such equipment along with other heavy equipment takes up as much as half of total operation cost of coal mining. Any un-anticipated mechanical failures on these equipment would not only results in high repair cost, but also high loss of production opportunity. Therefore, good maintenance system involving planning and execution, strengthened with the continuous improvement cycle is essential in order to increase the maintenance cost-effectiveness and in the same time, reliability and availability of the whole fleet of heavy equipment.

One of the company problems in their dump trucks is at their newly acquired electric dump trucks. With the net machine weight of about 180 ton, the electric truck has a payload capacity of 255 ton, or 435 ton in total. It is powered by a-2700 HP diesel engine producing power that drives two electric motor, each with the power of 1.25 MW serving each rear wheel-set. From 1480 rpm motor speed, a final drive with the total reduction ratio of 40.8 transmits the torque to the wheel-set. It consists of two stage planetary gears. On a number of occasions, PT KPC face mechanical failure problems in the final drive gears. Under normal load condition, the final drive broke down to pieces resulting in total break-down in production. The final drive set costs approximately USD 600,000 and requires long time to acquire. This, in turn, reduces the physical availability of the whole fleet, and causing even more loss of production opportunity to the company.

In order to find the root cause and possible recommendation to prevent such failures in the future, the authors and PT KPC conducted a failure analysis on this final drive. For the sake of confidentiality, the type and some data of the dump truck is deliberately concealed.

2. Methodology

The failure analysis activities starts from collecting data in forms of failed gear samples, relevant data and information regarding the final drive design as a reference for analysis. Beside that, any data and information on the operational and maintenance history/record are also collected in order to search for abnormality during its operational life. Visual examination is then carried out on the failed gears. The examination identifies the points of interest in search for

the failure mode(s) on the fracture surface. As an important stage in the investigation, a lateral thinking is needed to expand the possibilities of failure mechanism through cause and effect analysis, leading to cause and effect diagram, visualised in a "Fishbone diagram".

The analysis continues to a series of paralel activities, which includes both laboratory tests as well as simulation. The results of both analysis would be used in the root cause analysis, based on the fishbone diagram as above. The root cause of failure is found from the process along with the explanation of the most-likely failure mechanism. The above result is then discussed with PT KPC engineers as users in order to obtain input and furthermore, to formulate the recommended mitigation plan to prevent such failure from happening in the future.

The overall methodology is presented in Figure 1.

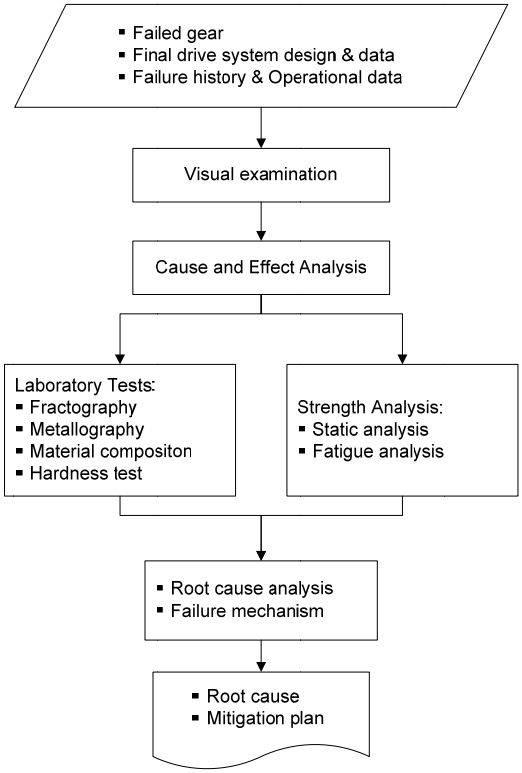

Figure 1 Failure analysis flow chart

3. Data Collected

Machine Data

The failure took place 2 months before the investigation, with no remains of the failed components available. The investigation is based on the secondary data with photographs of failed component. Only one part is observed, i.e. the failed 1st stage ring gear. The available data collected will be used as the source of information for the failure analysis.

Some important data of the dump truck is presented in Table 1. The final drive (Figure 2) transmits up to 1250 kW power direct from the electric motor to wheel rim for each wheel sets (right and left). Each consists of 2-stage of planetary gear with the total gear ratio of 40.8.

Table 1 Important specification of the dump truck [1]

Engine	**Electric motor**
Gross Power (SAE J1995): 2700 HP @1900 rpm Net power (SAE J1349): 2600 HP @1900 rpm Maximum Torque: 10 930 N.m @ 1 500rpm	Type: Four-pole, Three-phase, Asynchronous motor Rated: 1250 kW at 1480 rpm (max. 3465 rpm)
Final Drive	**Weight**
Type: Double planetary gear sets Total reduction ratio: 40.8:1 Max. speed: 56.2 km/h (34.9 mph)	Gross Max. Weight (GMW): 435,456 kg Net Machine Weight (NMW): 180,014 kg Payload (max.): 255,442 kg

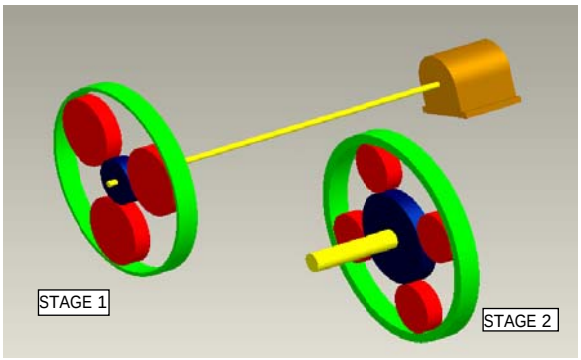

Figure 2 Final drive schematic assembly: 1st stage sun gear is linked to the electric motor, 1st stage ring gear is linked with 2nd stage sun gear, 2nd stage ring gear is fixed to the wheel rim. Adopted from the Truck service manual [2]

Load History

Loading history can be observed from the payload record for the machine that has gear failure. It is found that most of times, the truck was loaded 220 – 240 ton (86 – 94% of max. payload), and in a few occasions, it was overloaded to 320 ton (125 % max. payload).

Loading can also be observed from the terrain of the machine's operation. Here, the slope of the track is chosen as a good representation. From the track data served by the truck, it is found that mostly the slope at

Pit J, where the truck was operating, is noted to be 9 – 10%, with some area covering the slope by more than 10%. Maximum slope is not recorded.

These loading data shows that the machine was highly loaded with sometimes exceeding the maximum payload.

Oil Analysis Data

History on oil analysis is also available, since the company has a policy to sample the oil regularly and analysed by a third party company.

High particle count on the lubricant of the the truck (RH) was detected and the operation was stopped. It was revealed that the particle comes from the excessive wear on the planet bearing. The root cause is likely assembly fault. However, there was no notable sign on wear particle count in the truck (LH). The record shows rise in particle count, that is most likely due to running-in wear of newly assembled component. It should be normal later, otherwise other mode of failure would occur.

Visual Examination

Visual examination is carried out with unaided eye only on a failed component of the outer ring gear, whilst the rest is done through photographs. Further tests are required to confirm the conclusion of the preliminary failure analysis. Figure 3 shows preliminary pictures for visual examination.

Figure 3a is a picture taken by KPC engineers showing the failure of first stage ring gear before disassembled. It shows that one of the teeth of the ring gear breaks at its root, from one face to the other. It is estimated that this was the first failure. After disassembled (Figure 3b), it can be seen that: the breakage extents to the outer face of the ring gear; smooth beachmark is found towards the outer face as well as to the other face of the gear; Crack initiation is estimated as shown by the white arrow, by the location of the center of beachmark and the direction of the chevrons (grey arrow). The crack shape identification requires microscopic analysis, leading to the cause of crack, hence the failure.

4. Cause and Effect Diagram

In this failure analysis, the possible root causes are explored using fishbone diagram based on the possible tooth breakage failure modes as adopted from [3], i.e brittle fracture (Figure 4a), and fatigue failure (Figure 4b). Ductile fracture and surface failure are also common in the gear application, however not presented here since no indication of excessive wear and ductility was found on the gear or fracture surface.

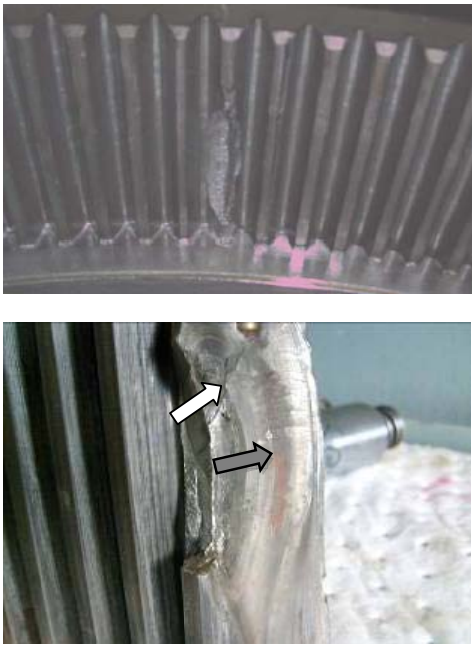

Figure 3 Visual examination, from top: First ring gear (attached), First ring gear (detached)

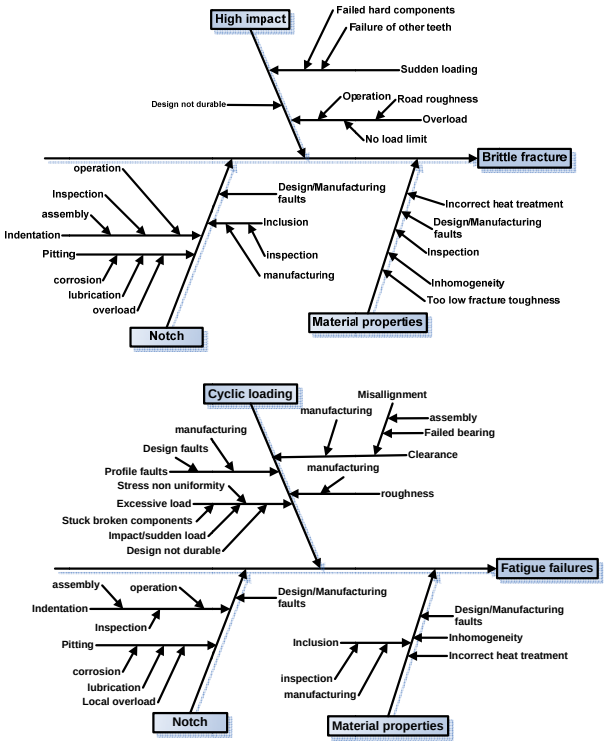

Figure 4 Cause & Effect Diagram: Brittle fracture, and fatigue fracture.

5. Material Examination

The material examination has been done on the broken first stage ring gear component as shown in Figure 5. The objective of the examination is to investigate from material's point of view the mode of failure.

Figure 5 Original specimen for material test.

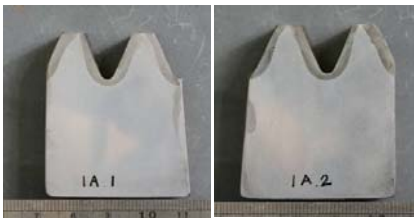

Figure 6 Two of the 6 test specimens.

The examinations that are carried out on the broken first stage ring gear, include: Fractography for fracture surface examination using stereo microscope; Optical Metallography for macrostructure and microstructure using optical microscope; Microhardness testing for measuring the hardness distribution using Micro-Vickers Hardness tester; Optical Emission Spectroscopy (OES).

The original specimen was cut using Electric Wire Cutting technique. It was then mounted, ground using sand paper, polished and etched for revealing the microstructure and macrostructure, as well as the microhardness measurement. There were six locations investigated, the sample result of which is shown in Figure 6.

From the optical metallography, the microstructure of each specimen are found. There are some small amount of inclusions present. Unfortunately, some inclusions happen to be close to each other as can be seen in Figure 7. The presence of inclusions at the size of up to 150 μm, which is close to one another will tend to increase the stress intensity factor, which is not good for the integrity of the gear.

The micro hardness measurement is carried out on three locations on each gear tooth sample, i.e. face area (location 1), root area (location 2) and tip area (location 3). The measurement results is presented in Figure 8. In general, the test shows that hardness of the face area has higher hardness compares to the root (location 2) and tip (location 3) areas. This is appropriate because the face area will endure friction force so that it will need a better wearability. On the other hand, the root area must have good toughness property because this area endures the highest stress. Therefore it would not be appropriate for the root area to have higher level of hardness. However, it can be seen from Figure 8, that the root hardness can reach almost 600 HV0.2, close to the surface area. The higher the hardness of the material, the lower will be its toughness. Therefore, it is undesireable for the tooth-root area to have higher hardness. At the root area, the combination of higher hardness due to inconsistent heat treatment that will result in lower fracture toughness and the presence of the unfavourable orientation and distribution of inclusions will create a damaging effect.

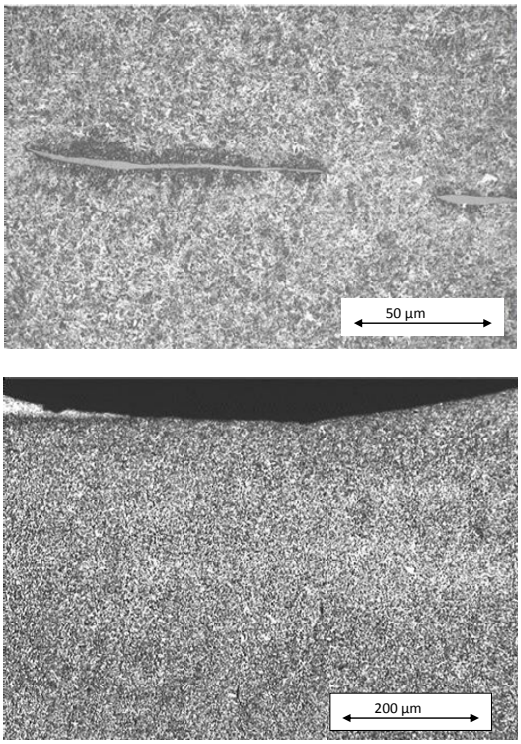

Figure 7 Examples of microstructure of the gear showing the presence and absence of inclusion.

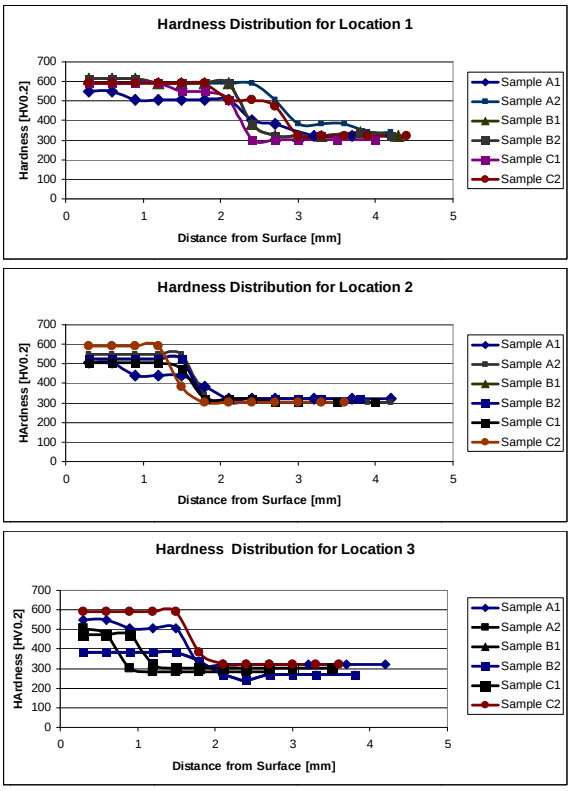

Figure 8 Micro-hardness test results for 6 specimens, on 3 locations: face, root and tip.

Table 2 Chemical composition of the specimen from OES, compared with the closest material standard [7]

	Specimen	**Ref. AIS1 4340**
%C	0.435	0.38-0.43
%Mn	0.72	0.60-0.80
%P	0.01	0.04 (max)
%S	0.02	0.04 (max)
%Si	0.26	0.20-0.35
%Ni	1.79	1.65-2.0
%Cr	0.80	0.70-0.90
%Mo	0.26	0.20-0.30

Finally, the material test includes the Optical Emission Spectroscopy (OES), that gives information on the chemical composition. As presented in Table 2, and by comparing with the closest material standard, it is found that the carbon content is slightly above the standard of AISI 4340 [7]. The higher carbon content will make the hardenability of the steel to be higher. It means that the hardening process will be able to create a deeper hard area. The effect of variation of the carbon percentage on the hardenability, hence the hardness of the material upon the same hardening process, can be seen in Figure 8. At the tooth-root, the combination of higher hardness due to inconsistent heat treatment that will result in lower fracture toughness and the presence of the unfavourable orientation and distribution of inclusions will create a damaging effect.

6. Simulation

The strength analysis is carried out to find the strength level of the gear component compared to the material properties against various operational loading case. First, static approach is used, with the shock load and other dynamic load is accommodated as amplification factor. The loading on the gear tooth is found based on kinematic relationship as well as the powertrain specification. Stress analysis is carried out, both using AGMA standard formulae and finite element software. The possible existence of cracks necesitates the use of static fracture mechanics approach to the strength analysis, in order to find the stress intensification factor generated by the crack compared with the fracture toughness of the material. Due to uncertain load history, accurate life prediction is difficult to be carried out.

Load Analysis

The main loading that is suspected to cause the first failure is due to gear tooth loading. Therefore, various loading case is predicted as follows, based on *normal* loading condition: 1) Maximum traction load at constant velocity, 2) Maximum motor torque, 3) Shock load. The first scenario represents the highest steady state (constant velocity) loading of one wheel according to the the truck performance charts [1], that is 1280 kN. With maximum wheel traction force, the required torque on the motor shaft is found 12.50 kNm, and the transmitted load at one ring gear tooth is 56.24 kN. The second scenario is found from the electric motor specification, that translates to motor torque of 24.19 kNm (after applying motor overload factor of 3) or a transmitted load of 108.84 kN. For rough mining application, it is suggested to have a shock loading factor of up to 3, that makes the third loading case, which translates to transmitted load at gear of 326.51 kN.

To describe the likelihood of the three loading cases above, a haul truck with maximum payload at constant speed will experience the loading not more than the maximum that the traction force the haul truck could deliver, otherwise the motor would stall. However, during the operation some dynamic effects occur, e.g. due to variation of road resistance, roughness of gear face etc. This load level could reach approximately 100% of load case (1) plus-minus 30% of dynamic loading, and comprises approximately 70-80% of the service life. A truck experiences transient mode when it accelerates from low or zero speed to a certain speed. The motor will deliver dynamic torque. This load case will form around 20% of the truck service life, depending on the

operation and very little chance reaching 300% of the rated torque (load case 2). On some occasions, the dynamic factors affect during transient mode, increasing the load level higher than load case 2. It is even slighter chance that the load level reach load case 3 under normal loading condition.

Beside the three most probable scenarios, there are additional scenarios that might happen, i.e. Additional load on the ring gear as well as abnormal loading, e.g. presence of large foreign object or stuck planet gears. The large amount of inertia from the moving haul truck with maximum payload will increase the loading greatly due to the above abnormalities. These cases has high uncertainty, therefore not to be taken into account.

AGMA Gear Stress

From the observation, tooth root breakage is found to be a major failure mode. Therefore, bending stress due to gear loading is calculated theoretically. The calculation is based on method by American Gear Manufacturers Association (AGMA) [4,5]. The AGMA bending stress is defined by,

$$\sigma_b = \frac{W_t.p_d.K_a.K_m.K_s.K_b.K_i}{F.J.K_v} \quad (1)$$

$$\sigma_c = C_p\sqrt{\frac{W_t}{F.I.d}\frac{C_a.C_m}{C_v}C_SC_f} \quad (2)$$

where, the nomenclature refers to AGMA as in Norton [5].

Finite Element Analysis

The analysis includes stress calculation on the tooth root, tooth surface, as well as simulating the stresses due to lateral loading on the ring gear. The geometric model is built, first a part of gear, with a single loading, i.e. due to maximum contact load. The second model use the whole ring gear, especially for simulating the lateral loading due to flexibility of the final drive assembly. The solid model was built on Solidworks 2005, whilst the finite element analysis was carried out using Ansys Workbench version 11.0. The finite element model can be seen in Figure 9.

Fracture Mechanics

When crack takes place conventional strength analysis will no longer applicable. Fracture mechanics approach should be used, wile the result from the above strength analysis is used to estimate the nominal stress as if no crack takes place. The analysis is divided into two types, i.e. static and fatigue analysis. In the static analysis, the *stress intensity factor* (SIF) is compared with the *fracture toughness*, i.e. a material mechanical property. Whilst, for fatigue analysis, more mechanical properties are required.

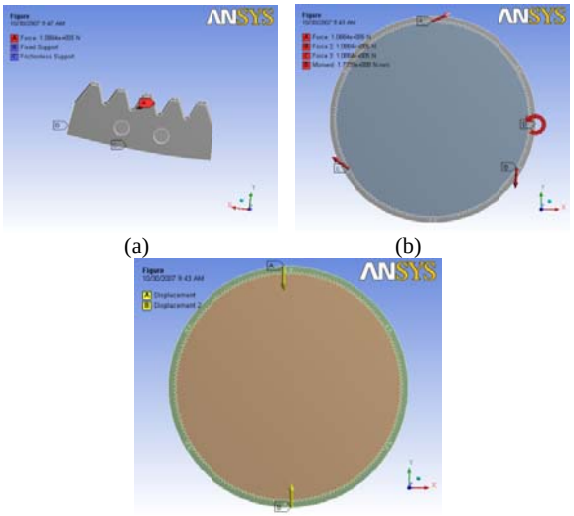

(a) (b)

(c)

Figure 9 FE Model: a) segmented gear, b) whole gear, c) whole gear model with lateral load

From the visual examination, it is clear that the major failure is due to fatigue. However, since the input data of cyclic loading is difficult to find accurately in unsteady speed application, as in the haul truck, and the mechanical properties for the particular component requires advanced tests, the extent of the current analysis will only be based on static analysis. It is safe to say that the initial failure is due to fatigue. The static analysis will estimate the loading that causes final fracture after crack propagation due to fatigue loading.

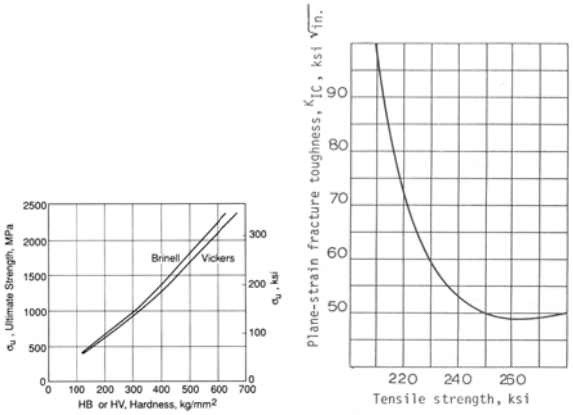

Figure 10 Material property relationship, from left: Hardness-UTS [8], and UTS and fracture toughness [9]

According to spectrometry test and after confirmed with the manufacturer, the gear material is known to be AISI4340. From micro-hardness tests on various locations, it is found that the hardness of the tooth is approximately 600 HV (Vickers) on the surface and 324 HV at the base material. The ultimate strength can be estimated, for surface and base material, respectively, 2070 MPa and 1000 MPa, according to Figure 10a [8].

Furthermore, the fracture toughness, K_{IC}, for the gear can be found from the relationship as in Figure 10b, i.e. 40 MPa $m^{1/2}$ (at the surface), and 180 MPa $m^{1/2}$ (base material).

For the formulation of stress intensity factor (SIF), the shape of flaw is deducted. It is suspected that the flaw in form of inclusion is either on the surface or internally, as found from the optical metallography test. Formulation below of can be used to model the plane strain stress intensity factor in an opening mode [9].

$$K_I = 2 \cdot S \cdot M_K \left(\frac{a}{Q} \right)^{1/2} \quad \text{for surface flaw} \tag{3}$$

$$K_I = S \left(\frac{\pi a}{Q} \right)^{1/2} \quad \text{for circular internal flaw} \tag{4}$$

Where:

S : Nominal stress, obtained from theoretical or finite element analyses (MPa)
M_K: back free-surface correction factor, a size factor
a : flaw length (m)
Q : Flaw shape parameter

Result and Analysis

For static strength analysis described previously, Table 3 shows the result of designed bending stress and surface stress based on AGMA formulae for the three loading cases defined previously. At a load corresponding to maximum motor torque, i.e. when accelerating at maximum payload, the bending stress is less than half the ultimate strength of AISI4340 material without hardening, or the safety factor is higher than 2. However, in the more unlikely event of shock load, there is a possibility that such loading causes overstress. This overstress (1184 MPa) could result in tooth breakage if the material is brittle due to hardening, especially if accompanied with material defects.

Table 3 AGMA bending stresses at tooth root and surface stress of ring gear

	σ_b (MPa)	σ_c (MPa)
Max. steady state	200.40	497.09
Max. motor torque	394.55	691.52
Max. shock load	1183.86	1197.73

Table 4 Comparison of FE Analysis results with AGMA prediction for bending stress at the tooth root for transmitted load of 108.84 kN

	σ_{root} (MPa)
Segmented model (FE)	358.47
Full gear model (FE)	301.53
Theoretical (AGMA)	395.51

Table 5 Results of FE analysis on various loading condition

	Root fillet	*Tooth root*
Max. stress due to single tooth load	180.56	151.02
Max. stress due to Gear lateral load	962.39	558.52
Max. stress due to combined load	971.66	663.04

Table 6 Critical flaw length for various loading cases (in mm)

	Surface	**ECD***	**internal**
Max. steady state	11.29	30.4	3355.56
Max. motor torque	6.13	7.84	865.69
Max. shock load	1.77	0.87	96.23

* ECD: Within Effective Case Depth (2.79 mm), a point sample that the flaw is in 2 mm deep.

From the finite element analysis, the principal stress is selected to be monitored, so that can be compared with the AGMA solution. The result for loading case 1 (tooth load only) can be compared between the two FE model, i.e. segmented and full ring gear in. The segmented model (Figure 9) gives the maximum principal stress of 358 MPa, whilst the full model gives 302 MPa for loading case 1, after a factor of 1.67 is applied due to load distribution. Comparison with the result of AGMA prediction is given in Table 4.

For the possible presence of defect in form of inclusion, as indicated from the metallography tests, static fracture mechanics approach is used, with the result as follows. With nominal stress obtained from the stress analysis, based on various loading cases as described previously, the critical flaw length can be calculated using Eqn. (3) and (4), with the result presented in Table 6.

It is shown that it requires large critical flaw length to cause the gear to fracture under static loading. However, in the least likely event of maximum shock loading or even abnormal loading, brittle fracture can certainly happen as it requires less than 1 mm flaw length (in the case of flaw within ECD). Flaw length larger than that can certainly result in tooth fracture in a lower load. Therefore, from the fracture mechanics analysis, the most likely cause of fracture is brittle fracture on surface or within ECD hardened part due to shock load or high abnormal loading condition with the existence of initial flaw/crack. This conforms to the finding from the failed component (Figure 7).

7. Summary of Analysis

Failure analysis on the ring gear is carried out on one half of the failed part not immediately after the failure. From the two perspectives, i.e. material examination and strength analysis, the overall result of analysis can be summarized as follows.

From fractography examination, it is found that the fatigue beachmark is initiated from the other half and form in two directions, i.e. through tooth thickness and through gear thickness (radillay). It is suspected that origin of failure is on the other half of the failed part, and the failure observed is a result of the second stage of failure. Metallography tests reveal the micro-structure of the gear material and show the presence of inclusions, with a size of approx. 150 micrometer. Gear material chemical composition is found using Optical Emission Spectroscopy (OES), and confirms that the material is of the AISI4340 standard material, with slightly higher carbon content detected. Micro-hardness tests show some variation of hardness and also shows that in some cases, surface hardening was done on the root too, which is quite inappropriate. The hardness is found up to be over 600 BHN on the surface and 324 BHN on the base material. These translates to ultimate strength of 2070 MPa and 1000 MPa for surface and base, respectively.

From load and static strength analysis, the load level and stresses on the gear can be predicted based on the defined load cases. It is concluded that the maximum normal load case, i.e. static loading with additional dynamic factors, would not cause the failures since it is below the ultimate strength (2070 MPa). Higher stress is estimated due to additional lateral loading, however still within the range of safe condition. And if failure occur due to lateral load, it would occur on the fillet bottom radially, instead of the tooth root and circumferentially.

The presence of flaw in form of inclusion, necessitates the use of fracture mechanics approach. Fracture mechanic analysis reveals that the maximum normal load cases may have caused the failure if initial flaw/crack took place. It is suggested that the critical length of any crack/flaw would be 1.77 mm.

8. Conclusion

The failure analysis is carried out not immediately after the failure. Some evidences, data and information are not completed. Examination is carried out only on one half of the failure parts. Secondary data is used from the photographs with limited accompanying data. Immediate data collection and visual examination/ observation would certainly help to obtain accurate failure analysis result. Nevertheless, based on the available data, facts and calculation, the above suspected failure mechanism can still be justified.

The root cause of the failure is suspected due to surface material on the root being too hard, accompanied with material flaw and under high impact tooth loading. Inlusion may have contributed to the formation of this flaw.

The presence of similar defect on the surface or subsurface of the tooth root with low fracture toughness is suspected to cause the first brittle fracture in the direction of the tooth thickness up to the middle of the tooth. The surface roughness left from the brittle fracture of the first failure became the initial crack of the second stage failures. The second stage of failure is in form of fatigue failure both through the tooth thickness and through the thickness of the gear (radially) before final fracture in both directions. Through-tooth-thikness failure was caused by bending stress, whilst failure in radial direction was caused by suspected lateral load due to the overall flexibility of the 1st stage ring gear asembly. Finite element analysis result shows that the second stage failure cannot occur without the presence of the first stage failure.

9. Recommendation

The mitigation strategy includes preventing such failure from happening as well as early detecting the failure in order to prevent further damage and loss to the operation. From the review of alternatif actions related various stages of the component life-cycle, including design, manufacturing, quality control, commissioning, operation, maintenance and monitoring/inspection, mitigation plan is recommended concerning, mainly in manufacturing stage and inspection during operational, as follows.

- Improvement on the heat treatment technique and process, including higher control of carbon percentage and hardening profile.
- Early detection on tooth breakage can be carried out by observing the vibration of the final drive, i.e. by running the wheels with rear wheels jacked-up on constant speed. This action plan can be applied during the existing maintenance/regular maintenance.

References

[1] Dump Truck Equipment, Dimensions and Specification
[2] Dump Truck Service manual
[3] Tallian, T.E., Failure atlas for Hertz contact machine elements, ASME Press, New York, 1992.
[4] AGMA (American Gear Manufacturer's Association) standards
[5] Norton, R.L., Machine design, an integrated apporach, Prentice-Hall, New Jersey, 1998
[6] Aswani, K.G., A Text Book of Material Science, S. Chand & Co., 2001
[7] Callister, W.D., Material science and engineering: an introduction, 4th ed., John Wiley & Sons, Toronto, 1997
[8] Dowling, N.E., Mechanical behaviour of materials, Prentice-Hall Int., New Jersey, 1993.
[9] Blake, A, Practical fracture mechanics in design, Marcel Dekker Inc., New York, 1996